

Melting of the vortex-solid in irradiated $\text{Bi}_2\text{Sr}_2\text{CaCu}_2\text{O}_{8+\delta}$ single crystals in tilted magnetic fields

Jovan Mirković¹, Sergey Savel'ev^{2,3}, Hirokazu Sato¹,
Franco Nori^{2,4} and Kazuo Kadowaki¹

¹ Institute of Materials Science, The University of Tsukuba,
1-1-1 Tennodai, Tsukuba, 305-8573, Japan

² Frontier Research System, The Institute of Physical and
Chemical Research (RIKEN), Wako-shi, Saitama, 351-0198, Japan

³ Department of Physics, Loughborough University,
Loughborough LE11 3TU, UK

⁴ Department of Physics and MCTP, The University of Michigan,
Ann Arbor, MI 48109-1040, USA

E-mail: ssavelev@riken.jp

New Journal of Physics **8** (2006) 226

Received 22 July 2006

Published 5 October 2006

Online at <http://www.njp.org/>

doi:10.1088/1367-2630/8/10/226

Abstract. We study the boundary between the vortex-solid and the vortex-liquid phases in the H_c-H_{ab} plane, for irradiated $\text{Bi}_2\text{Sr}_2\text{CaCu}_2\text{O}_{8+\delta}$ single crystals, by measuring the ac-local magnetic permeability in tilted magnetic fields. For high temperatures and at the phase boundary, we find that the c -axis magnetic field component H_c^{trans} decreases linearly when increasing the in-plane magnetic field H_{ab} , surprisingly in a wider angular range than in pristine samples. Strikingly, at lower temperatures, this linear decrease of $H_c^{\text{trans}}(H_{ab})$ transforms to a concave, hyperbolic-like, curve that differs even more strongly from the usual Ginzburg–Landau (GL) elliptical phase boundary. We also propose a theoretical approach to solve this puzzle.

Contents

1. Introduction	2
2. Experiment	3
3. Vortex dynamics near the vortex-solid–vortex-liquid boundary	7
4. Theoretical interpretation	8
5. Conclusions	11
Acknowledgments	11
References	12

1. Introduction

Vortex matter in strongly anisotropic layered superconductors, such as $\text{Bi}_2\text{Sr}_2\text{CaCu}_2\text{O}_{8+\delta}$ single crystals, drastically differs from vortex lattices in moderately anisotropic superconductors, e.g., $\text{YBa}_2\text{Cu}_3\text{O}_{7-\delta}$. In tilted magnetic fields, $\text{Bi}_2\text{Sr}_2\text{CaCu}_2\text{O}_{8+\delta}$ samples have two types of vortices: the c -axis component H_c of the magnetic field produces stacks of quasi-two-dimensional (2D) pancake vortices (PVs) [1], while the in-plane field component H_{ab} generates Josephson vortices (JV) in the layers between the CuO_2 planes [2]. Interacting crossing PV and JV lattices have been intensively studied theoretically [3]–[8] and recently directly observed using Lorentz microscopy [9, 10], scanning Hall probe microscopy [11], and magneto-optical imaging [12].

Crossing vortex lattices exhibit non-trivial and fascinating dynamical behaviour (see, e.g., [13, 14]) which allows us to manipulate [15]–[17] one vortex lattice via another one, as well as non-standard thermodynamic properties [18]–[22]. For instance, in contrast to the Ginzburg–Landau (GL) approach, the first-order melting transition line (the boundary separating the vortex-solid and vortex-liquid phases) exhibits a ‘step-wise’ shape [20, 23] (i.e., approximately linear decay interrupted by two flat-plateaux) if plotted in the H_c – H_{ab} plane. Namely, the c -axis component H_c^{trans} at the phase transition decays linearly when increasing H_{ab} , followed by a plateau (i.e., a very weak H_{ab} -dependence of H_c^{trans}). A similar stepwise shape of the phase boundary was observed [19, 21] at a much lower temperature, $T = 35$ K, where disorder plays an essential role and the transition is smooth—in contrast to first order. Thus, this suggests that the shape of the transition line is controlled by general thermodynamic properties, rather than the precise statistical features of the vortex-solid-phase, including vortex-glass, Bragg-glass, or Bose-glass. Note that the difference between these glass phases is usually hardly distinguishable in experiments.

This paper focuses on the important issue of how disorder affects vortex matter. Specifically, our main goal is to obtain the boundary separating the ‘vortex solid’ with lower resistivity (hereafter called ‘vortex-solid’) and the ‘vortex phase’ (denoted as ‘vortex-liquid’) with higher resistivity in heavy-ion-irradiated $\text{Bi}_2\text{Sr}_2\text{CaCu}_2\text{O}_{8+\delta}$ samples in tilted fields. We performed measurements of the phase boundary of irradiated $\text{Bi}_2\text{Sr}_2\text{CaCu}_2\text{O}_{8+\delta}$ through the whole angular range. Irradiation expands the vortex-solid-phase along all directions, while simultaneously decreasing the anisotropy of the material, i.e., making the resistive properties of the measured samples more isotropic than in a pristine sample. Note that the suppression of the detrimental high material anisotropy in $\text{Bi}_2\text{Sr}_2\text{CaCu}_2\text{O}_{8+\delta}$ by columnar defects is consistent with earlier studies [24]–[26]. We find that, at relatively high temperatures, the c -axis component of the

transition field H_c^{trans} decreases linearly when increasing the in-plane magnetic field H_{ab} , as for pristine samples [18, 20]. At low temperatures, the linear decay is replaced by a concave, hyperbolic-like, curve that differs even more from the elliptical transition lines [27] for moderately anisotropic materials. This is striking because such a phase boundary shape has never been observed so far, and cannot be described by the standard theories: the usual GL phase boundary has elliptical shape, while the model in [5] for the crossing vortex lattices provides a linear decay in $H_c^{\text{trans}}(H_{\text{ab}})$.

Note that the recent surge [28] of interest in studies of anisotropic layered superconductors, including $\text{Bi}_2\text{Sr}_2\text{CaCu}_2\text{O}_{8+\delta}$ compounds, is due the expectation to obtain terahertz radiation from moving JV lattices and to develop a set of well-integrated terahertz devices including terahertz filters, detectors, amplifiers etc.

2. Experiment

In order to study the important problem of the effect of disorder on vortex matter in magnetic fields with arbitrary orientation, we used two $\text{Bi}_2\text{Sr}_2\text{CaCu}_2\text{O}_{8+\delta}$ as-grown single crystals [29] (with $T_c = 89$ and 88.9 K). These samples had defects introduced by heavy-ion irradiation ($^{127}\text{I}^{28+}$, 650 MeV), with doses of $B_\Phi = 0.1$ and 0.02 T, respectively. The incident beams were directed along the c -axis. Since the defects were produced by low-energy ions (compare, for instance, with the 5.8 GeV radiation used in [26] to create columnar defects), we could expect some ‘bent columnar’ defects due to deviations of ions from straight trajectories when passing through $\text{Bi}_2\text{Sr}_2\text{CaCu}_2\text{O}_{8+\delta}$ crystals with thickness of about $20 \mu\text{m}$. Thus, we can expect less correlated pinning in our samples with respect to samples with standard columnar defects. The vortex phases were probed via local ac mutual-inductance measurements by using a set of two miniature coils. One coil generated the local magnetic field to excite the vortex system, while the second coil was glued on the other side of the samples in order to detect the transmitted ac response. The size of the coils was 0.35 mm, which was sufficiently smaller than the size of the samples (~ 3 mm \times 3 mm). This coil design was developed in order to diminish the surface barrier [30] and to probe bulk properties. Indeed, even though some fraction of the current generated by the coil can flow near the sample edge due to the surface barrier, the pick-up coil was well-screened from these peripheral currents and it mostly measured the current directly under the coil. Since the coils were fixed on the sample, the sensitivity for all \mathbf{H} directions was kept constant, even when \mathbf{H} was exactly parallel to the ab -plane. The dc magnetic field, generated by a 70 kOe split coil magnet, was rotated with a fine angular resolution of 0.01° . A representative set of data (ac-local magnetic permeability versus dc magnetic field for different angles) is shown in figure 1. The curves are smooth, with no sign of the sharp features attributed to the first-order vortex lattice melting transition that was observed earlier in a pristine $\text{Bi}_2\text{Sr}_2\text{CaCu}_2\text{O}_{8+\delta}$ sample [31]. Therefore, in order to construct the phase boundary (see figures 2 and 3), we used the voltage level of $15 \mu\text{V}$ (approximately middle point between zero and the saturation value of the real part of the permeability, μ' , figure 1), in analogy with the definition of the irreversibility line.

We would like to stress that a voltage criterion is usually in good agreement with other definitions of vortex-liquid–vortex-solid boundary. For instance, the article [26] contains a comparison of the phase boundary measured by two methods: (i) using a voltage criterion, and (ii) using the criterion of the appearance of nonlinearity attributed to the vortex-solid phase.

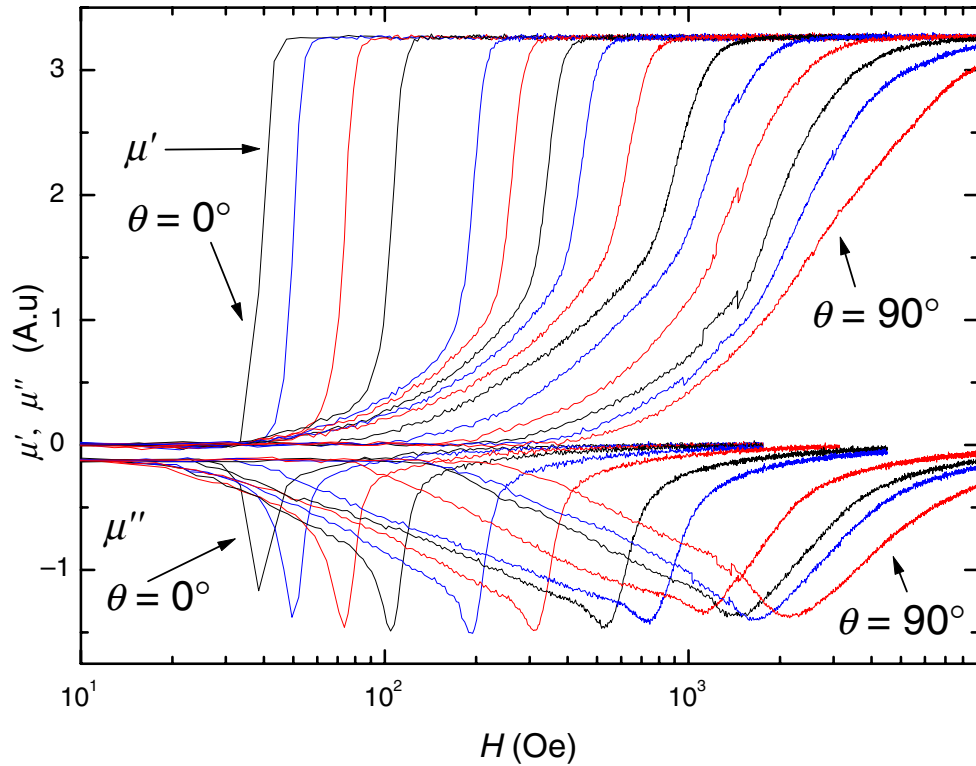


Figure 1. The magnetic field dependence of the real μ' and imaginary μ'' parts of the ac-local magnetic permeability μ for irradiated $\text{Bi}_2\text{Sr}_2\text{CaCu}_2\text{O}_{8+\delta}$, with a dose $B_\Phi = 0.1$ T. Measurements were at $T = 85.2$ K for various field orientations with respect to the c -axis.

Of course, determining the location of the phase boundary for the continuous phase transition observed here is a delicate issue. Indeed, the line (associated with the phase boundary) measured by using the voltage criterion depends on both this criterion and also the amplitude and frequency of the applied signal. Changing these parameters, we have obtained a set of slightly different lines. However, the shape of all the lines is almost the same, i.e., does not depend on a voltage criterion and the strength of the applied signal. Thus, the ‘phase boundary’ terminology used below refers to the measured shape of this phase line rather than the precise location of the solid–liquid transition.

The phase diagram for strongly ($B_\Phi = 0.1$ T) irradiated $\text{Bi}_2\text{Sr}_2\text{CaCu}_2\text{O}_{8+\delta}$ at the higher temperature $T = 88$ K exhibits a behaviour (figure 2(a)) which is somewhat similar to the stepwise phase boundary obtained earlier for non-irradiated samples (inset of figure 2(a)). Namely, the linear decay of H_c^{trans} , when increasing the in-plane magnetic field H_{ab} , transforms to a very weak (plateau) dependence of H_c^{trans} . However, for the strongly irradiated sample shown in figure 2(a), the linear decrease of $H_c^{\text{trans}}(H_{\text{ab}})$ occurs for a much larger region of phase diagram (than for pristine samples, see e.g., [20, 31] or inset of figure 2(a)), persisting up to higher H_{ab} and lower H_c . The effective anisotropy γ (i.e., the elongation of the phase boundary when \mathbf{H} rotates from $\mathbf{H} \parallel \mathbf{c}$ to $\mathbf{H} \parallel \text{ab}$) could be estimated as $\gamma = \max(H_c^{\text{trans}}) / \max(H_{\text{ab}}) \approx 67.5$ which is much smaller than for non-irradiated samples (≈ 150 obtained in [23]).

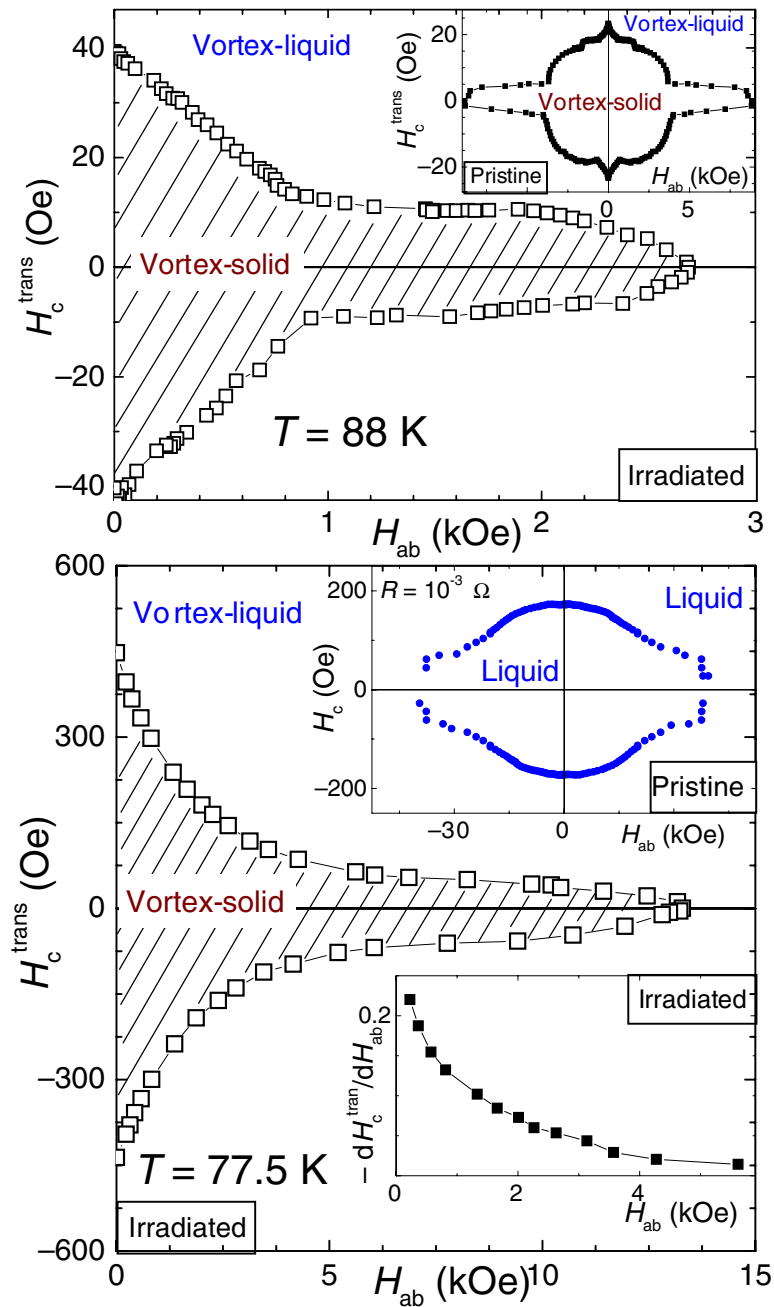


Figure 2. Phase boundary between vortex-solid and vortex-liquid phases in the H_c - H_{ab} plane of strongly ($B_\Phi = 0.1 \text{ T}$) irradiated $\text{Bi}_2\text{Sr}_2\text{CaCu}_2\text{O}_{8+\delta}$, at two different temperatures of 88 (a) and 77.5 K (b). The linear decrease (a) of $H_c^{\text{trans}}(H_{ab})$ observed for high temperatures changes to a concave (b), hyperbolic-like, behaviour of $H_c^{\text{trans}}(H_{ab})$ at lower temperatures. Inset in (a): same as in panel (a), but for a non-irradiated sample [23]. Upper inset in panel (b): vortex-liquid equi-resistance contour at $T = 86.6 \text{ K}$, obtained for non-irradiated $\text{Bi}_2\text{Sr}_2\text{CaCu}_2\text{O}_{8+\delta}$ single crystals in [23] and shown here for comparison. Lower inset in panel (b): the slope of the phase line $dH_c^{\text{trans}}/dH_{ab}$ as a function of H_c . This slope is proportional to the JV energy and decreases when H_c increases.

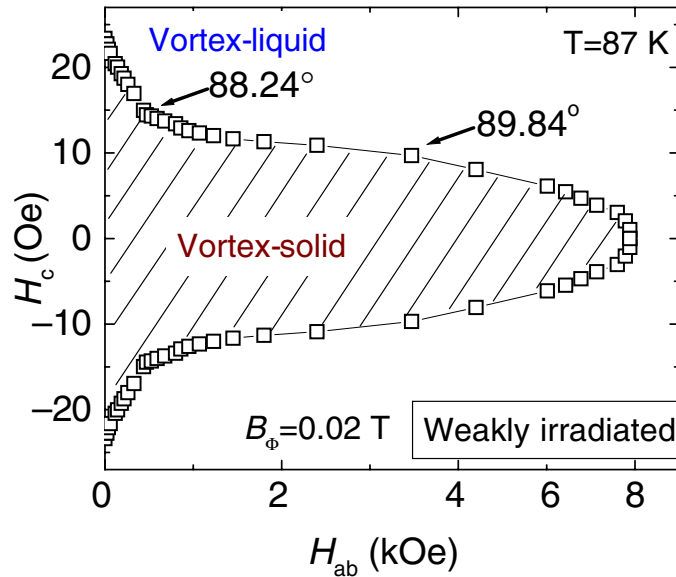


Figure 3. Phase boundary between vortex-solid and vortex-liquid phases in the H_c – H_{ab} plane for weakly irradiated $\text{Bi}_2\text{Sr}_2\text{CaCu}_2\text{O}_{8+\delta}$, at $T = 87$ K and $B_\Phi = 0.02$ T. The gradual evolution with increasing irradiation dose can be easily seen by comparing this figure with the main panel of figure 2(b): the sharp transition from the linear decay of $H_c^{\text{trans}}(H_{ab})$ to a very weak dependence observed for pristine samples (see, e.g., in the inset of figure 2(a)) is now replaced by a smooth transition (a concave piece of the curve in the figure shown above) between linear decay and weak dependence in $H_c^{\text{trans}}(H_{ab})$.

The introduced effective anisotropy is applicable only to estimate the elongation of the measured phase boundary, i.e., the line obtained using the chosen voltage criterion. Because the melting fields along the ab -plane and the c -axis have different temperature dependences [32] (due to different critical exponents), such an anisotropy also depends on temperature and clearly cannot be used to describe vortex systems within the GL theory. However, such a phenomenological anisotropy parameter still provides some insight into the anisotropy of vortex matter in irradiated $\text{Bi}_2\text{Sr}_2\text{CaCu}_2\text{O}_{8+\delta}$ samples. Indeed, this anisotropy decreases with increasing the radiation dose, consistent with previous studies of irradiated $\text{Bi}_2\text{Sr}_2\text{CaCu}_2\text{O}_{8+\delta}$ samples [24]–[26].

For the lower temperature 77.5 K, pinning becomes stronger and, as shown in figure 2, the transition line changes drastically: the linear part in figure 2(b) (which can be considered a fingerprint of a crossing vortex lattice) transforms to a concave, hyperbolic-like, curve in figure 2(b). Thus, at these lower temperatures, the question arises: is it still a crossing vortex lattices (i.e., the interpenetrating PV and JV lattices controlled by out-of-plane and in-plane magnetic fields, respectively) or something different?

It is important to stress that quick changes in thermodynamic properties at the transition between liquid and solid vortex phases results in this very unusual concave shape of the phase boundary, rather than a gradual evolution of the properties within each vortex phase. In order to analyse this, we consider the equiresistance contour deep in the liquid phase studied earlier in [23] for pristine samples. This contour is not a phase boundary and it is completely determined

by properties of the vortex-liquid. However, these contours allow us to make a link between experimental data and the commonly used GL theory. According to scaling law [27], the resistivity in a magnetic field H , tilted away from the c -axis for the angle θ , depends only on the reduced field as

$$\rho(H, \theta) = \rho \left(H \sqrt{\cos^2 \theta + \sin^2 \theta / \gamma^2} \right). \quad (1)$$

Thus, for an equiresistance contour, we obtain the elliptical shape

$$H_c^2(\theta) + H_{ab}^2(\theta) / \gamma^2 = H_c^2(\theta = 0). \quad (2)$$

Indeed, it was found [23] that such an equiresistance line shows an almost elliptical behaviour (except for a very narrow angular region near the ab -plane) and, thus, can be roughly described using a 3D GL theory with appropriate temperature dependence for the effective anisotropy. Using the same scaling rules [27], we derive the elliptical shape for vortex-solid–vortex-liquid transition. However, in strong contrast to the behaviour [23] in the vortex-liquid, the phase boundary between vortex-liquid and vortex-solid for the irradiated sample shows a concave phase line (a hypocycloid with four cusps) at the lower temperature $T = 77.5$ K. These properties are robust for various criteria of the definition of the phase boundary.

We have also measured the vortex-solid melting transition (figure 3) for a weakly irradiated sample with $B_\phi = 0.02$ T at a temperature $T = 87.5$ K ($T_c = 88.9$ K). This sample shows an intermediate behaviour between the pristine and strongly irradiated samples discussed above. As for pristine samples, the linear decay of $H_c^{\text{trans}}(H_{ab})$ at low in-plane fields is still clearly seen for this weakly irradiated sample. However, a change from a linear decrease of $H_c^{\text{trans}}(H_{ab})$ to a plateau occurs via a piece of the concave curve which smears out the sharp (point-like) change from the linear decay to the plateau in $H_c^{\text{trans}}(H_{ab})$. This offers a picture of how the stepwise shape of the vortex lattice melting transition transforms to an unusual hypocycloid shape of the vortex-solid melting transition for strongly irradiated samples.

Thus, we can conclude that the phase boundary is influenced by the irradiation dose: the concave shape occurs only for a sufficiently large dose when the density of pinning centres is much higher than the vortex density. In this case, according to [26], 2D PVs form 3D vortices which can slightly bend to adjust to the pinning potential.

3. Vortex dynamics near the vortex-solid–vortex-liquid boundary

In order to interpret the obtained results, we combine

1. The ‘discrete’ superconductor model [26] proposed for the vortex-solid–vortex-liquid phase transition in a superconductor with columnar defects and
2. the model [5, 20] employing crossing vortex lattices to describe the vortex lattice melting transition in a pure superconductor in tilted magnetic fields.

The model [26] successfully describes experiments for $H \parallel c$. According to this model [26], the vortex-solid(Bose-glass)–vortex-liquid phase transition occurs when the diffusion of PVs starts between different PV stacks trapped by columnar defects. This is similar to the unbinding of dislocations in moderately anisotropic superconductors. Such diffusion (i.e., jumping of PVs

between different vortex lines) results in a strong suppression of the Josephson coupling in the vortex-liquid phase. A similar suppression of the Josephson coupling in the vortex-liquid was proposed by Koshlev [5] when deriving the vortex lattice melting transition boundary in pristine superconductors. Consistent with both of these models, below we assume zero Josephson coupling in the vortex-liquid.

As shown in [26], the elasticity starts to play a crucial role if two conditions are valid:

$$H_c > \Phi_0/(\lambda_{ab}^2 + \gamma^2 s^2)^{1/2} \sim 50 \text{ Oe}, \quad (3)$$

and

$$H_c > B_\Phi/6 \sim 150 \text{ Oe}. \quad (4)$$

This is the case for our measurements. Thus, we have to take into account elastic energies. Analysing different contributions to the elastic energy, it was shown [5] that the tilted energy U_{44} is only relevant (and will be taken into account below) for strongly anisotropic superconductors in this magnetic field range.

Finally, we assume that PVs can only occupy discrete positions associated with pinning centres, in agreement with the discrete superconductor model [26]. These discrete positions are randomly distributed, which is correct for both straight columnar defects and even more appropriate for the bent columnar defects occurring due to deviations of ions having relatively low energy (which likely happens in our case).

This general conclusions allow us to propose a model for a qualitative description of the vortex-solid–vortex–liquid transition line (see next section).

4. Theoretical interpretation

Now we discuss the thermodynamics responsible for the evolution of the vortex-solid–vortex-liquid phase boundary of the irradiated $\text{Bi}_2\text{Sr}_2\text{CaCu}_2\text{O}_{8+\delta}$ samples when the temperature decreases. The free energy of crossing lattices can be written as [5, 20]: $F^{\text{solid}}(H_c, H_{ab}) = \mathcal{F}_0^{\text{solid}}(H_c) + H_{ab}^2/8\pi + \epsilon_J H_{ab}/\Phi_0$. It consists of the free energy of the PV lattice $\mathcal{F}_0^{\text{solid}}(H_c)$ at zero in-plane field, the in-plane magnetic energy, and the energy of the JV lattice, where ϵ_J is the energy of a JV. Following approaches in [5, 20], we can assume that the Josephson coupling is very small in the vortex-liquid phase, due to large thermal fluctuations and/or diffusion of PVs between PV stacks (i.e., $\epsilon_J \approx 0$). Thus, for a qualitative analysis, we can approximate the free energy in the vortex-liquid phase as $F^{\text{liquid}}(H_c, H_{ab}) = \mathcal{F}_0^{\text{liquid}}(H_c) + H_{ab}^2/8\pi$, where $\mathcal{F}_0^{\text{liquid}}(H_c) = F^{\text{liquid}}(H_{ab} = 0)$ is the free energy of the vortex-liquid for zero in-plane fields. The condition that the free energy F^{solid} is equal to F^{liquid} at the phase boundary results in the following equation [5, 20] for the phase transition line:

$$H_c^{\text{trans}} = H_c^{\text{trans}}(H_{ab} = 0) - \frac{\epsilon_J}{\Phi_0(\Delta M)} H_{ab}, \quad (5)$$

where $\Delta M = \partial(\mathcal{F}_0^{\text{solid}} - \mathcal{F}_0^{\text{liquid}})/\partial H_c$.

For *irradiated* samples, the experimentally observed concave shape of the transition line suggests that the energy ϵ_J of a JV decays when H_c decreases. Indeed, the slope of the transition

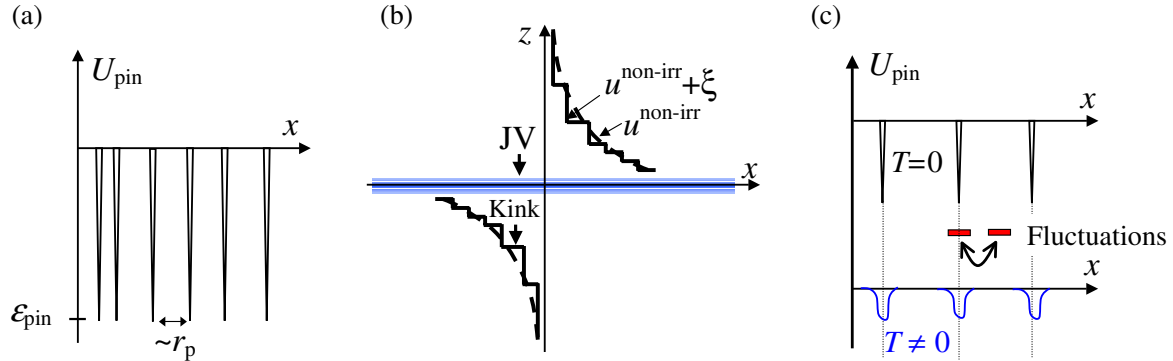


Figure 4. (a) schematically shows a potential describing columnar random pinning. (b) Schematic displacement of PVs in pristine ($u^{\text{non-irr}}$, smooth dashed lines) and in the irradiated ($u^{\text{non-irr}} + \xi$, step-like solid lines) samples occurring due to PV–JV interaction (a JV is shown in blue). (c) schematically illustrates how the $T = 0$ pinning potential effectively becomes smoother (in blue) due to thermal fluctuations: one pancake (thick red bar) is schematically shown fluctuating in and out of a pin, producing a smearing of the pinning potential.

line $H_c^{\text{trans}}(H_{\text{ab}})$, which is proportional to ε_J (see, equation (5)), decreases when lowering H_c (see, lower inset of figure 2(b)). Note that, as was derived in [5, 6], for pristine samples, the JV energy ε_J increases when decreasing H_c . This emphasizes the crucial role of the columnar defects on the thermodynamics of JVs and PVs.

For a pristine sample, the in-plane current generated by a JV displaces PVs a distance $u^{\text{non-irr}}$ from their unperturbed positions in a triangular lattice. This displacement $u^{\text{non-irr}}$ occurs mainly along a JV (along the x -axis) and decreases from the JV centre in both the out-of-plane (z) and in-plane (y) directions (see figure 4). The bending $\partial u^{\text{non-irr}}/\partial z$ of the PVs along a JV partly screens [6] the field of a bare JV. The displacement $u^{\text{non-irr}}$ and the effective JV field b_J can be derived from the force balance of the Lorentz force and the elastic restoring force. These can also be derived by minimizing the free energy functional $F_{\text{JV}}^{\text{non-irr}}(u)$ consisting of both the elastic tilt energy of PVs and the energy describing the interaction of PVs with the in-plane currents of the JV. The JV energy for pristine samples within such an approach [5, 6] is

$$\varepsilon_{\text{JV}}^{\text{non-irr}} = F_{\text{JV}}^{\text{non-irr}}[u^{\text{non-irr}}] = \frac{\Phi_0}{8\pi} b_J(z \approx s, y \approx \gamma^{\text{eff}} s) \propto \frac{1}{\sqrt{H_c}}, \quad (6)$$

with the effective anisotropy parameter γ^{eff} .

For irradiated samples, interactions of PVs with columnar defects should be taken into consideration. This decreases the energy of the vortex-solid at low temperatures (when thermal fluctuations are weak) as $\mathcal{F}_0^{\text{solid}} - \varepsilon_{\text{pin}} H_c / \Phi_0$ with the depth ε_{pin} of the pinning wells. Such a decrease of the free energy of the vortex-solid phase explains the experimentally observed high c -axis transition field $H_c^{\text{trans}} \sim 500$ Oe at $T = 77.5$ K (figure 2(a)). Moreover, the interaction of PVs with columnar defects has to be added to the force balance when we derive the displacement of PVs by JV currents. As a result, the free energy functional for a JV in an irradiated sample can be written as

$$F_{\text{JV}}[u] = F_{\text{JV}}^{\text{non-irr}}[u] + \frac{H_c}{\Phi_0} \int d^3r (U_{\text{pin}}(u) - \varepsilon_{\text{pin}}), \quad (7)$$

where U_{pin} is a random pinning potential (see figure 4(a)). The displacement $u^{\text{non-irr}}$ minimizes the energy functional $F_{\text{JV}}^{\text{non-irr}}$, but not the whole energy F_{JV} because of the pinning contribution. The functional F_{JV} takes its minimum value ε_{JV} , if PVs occupy the pinning potential minima which are nearest to the line $u^{\text{non-irr}}(y, z)$ (see, figure 4(b)). Next, we use the ‘discrete’ superconductor model [26], which assumes that the PVs only occupy the discrete positions of the pinning centres. Thus, the displacement u^{irr} can be approximated as

$$u^{\text{irr}} = u^{\text{non-irr}} + \xi, \quad (8)$$

where ξ is the displacement from $u^{\text{non-irr}}$ to the nearest pinning centre. For a random distribution of columnar defects, ξ is a random function with dispersion $\langle \xi^2 \rangle \sim r_p^2 \equiv \Phi_0/B_\Phi$. This results in an estimate of the JV energy:

$$\varepsilon_{\text{JV}} = F_{\text{JV}}^{\text{non-irr}}[u^{\text{non-irr}} + \xi] \approx \varepsilon_{\text{JV}}^{\text{non-irr}} + U_{44}r_p^2 S_c. \quad (9)$$

Here, the electromagnetic tilt energy can be estimated [5] as $U_{44} = \Phi_0 H_c \ln(\gamma s/\lambda_{\text{ab}})/(16\pi^2\lambda_{\text{ab}}^4)$, and S_c is the effective area where the JV currents are strong enough to shift the PVs away from the pinning centres (very roughly $S_c \lesssim \pi\gamma\lambda_{\text{ab}}^2$). The precise calculation of S_c is a rather difficult problem and will be discussed elsewhere. Nevertheless, if we assume that S_c is roughly constant with respect to H_c , we obtain

$$\varepsilon_{\text{JV}} \propto H_c + \beta H_c^{-1/2}, \quad (10)$$

and ε_{JV} could decrease with H_c for a certain region of parameters in agreement with experimental findings. Note that the suppression of the energy ε_{JV} of a JV also occurs when H_{ab} increases. However, the dependence of ε_{JV} on H_{ab} is very weak (logarithmic dependence) and can be ignored compared to the other effects studied above.

Another possible scenario is related to the smoothing of the transition from the vortex-solid to the vortex-liquid phase (from first to second order). In that case,

$$\frac{\partial \mathcal{F}_0^{\text{solid}}}{\partial H_c} \approx \frac{\partial \mathcal{F}_0^{\text{liquid}}}{\partial H_c}, \quad (11)$$

and the expansion of the vortex-solid and vortex-liquid free energies, $\mathcal{F}_0^{\text{solid}}$ and $\mathcal{F}_0^{\text{liquid}}$, up to the second order with respect to $(H_c^{\text{trans}}(H_{\text{ab}} = 0) - H_c^{\text{trans}}(H_{\text{ab}} \neq 0))$ must be done to obtain the transition line. In this approach, we derived the equation

$$H_c^{\text{trans}} \approx H_c(0) - \alpha \sqrt{H_{\text{ab}}}, \quad (12)$$

instead of the usual transition line (equation (5)). Here,

$$\alpha \approx \frac{2\varepsilon_{\text{J}}}{\Phi_0} \left[\frac{\partial^2 (\mathcal{F}_0^{\text{liquid}} - \mathcal{F}_0^{\text{solid}})}{\partial H_c^2} \right]^{-1}. \quad (13)$$

Equation (12) also describes the concave shape of the transition line.

At higher temperatures, the *pinning is smeared out* due to thermal fluctuations (see figure 4(c)) and the ‘discrete’ superconductor model [26] is no longer valid. As a result, the more *standard phase diagram* in H_c-H_{ab} plane is recovered. However, this thermally smoothed columnar pinning can still stabilize the distorted crossing lattices with respect to the formation of both a ‘crystal+chain’ vortex state and a ‘tilted vortex lattice’, when \mathbf{H} approaches the ab-plane. This explains the persistence of the linear decrease of $H_c^{\text{trans}}(H_{ab})$ for irradiated $\text{Bi}_2\text{Sr}_2\text{CaCu}_2\text{O}_{8+\delta}$ samples, compared to pristine samples. Indeed, the transformation of the linear decrease of H_c^{trans} to a weak dependence of $H_c^{\text{trans}}(H_{ab})$ is usually ascribed [6, 33] to the transition from a crossing vortex lattice to a tilted vortex lattice (or chain state). Thus, a very long (practically up to $\mathbf{H} \parallel \text{ab}$) linear decay of $H_c^{\text{trans}}(H_{ab})$ indicates that the tilted lattice phase is almost gone for the irradiated $\text{Bi}_2\text{Sr}_2\text{CaCu}_2\text{O}_{8+\delta}$ samples.

Here, we only provide a physical picture for calculating thermodynamic properties for irradiated $\text{Bi}_2\text{Sr}_2\text{CaCu}_2\text{O}_{8+\delta}$ samples. For a quantitative description, a more detailed and cumbersome theory should be developed, that properly considers the PV kink energy (see, figure 4(b)), nonlocal effects [34], and kinetics [35] of vortices with different orientations, among others.

Finally, we address the issue of what kind of vortex phase could exist in strongly irradiated $\text{Bi}_2\text{Sr}_2\text{CaCu}_2\text{O}_{8+\delta}$ samples. Comparing the well-known scaling of current-voltage (IV) curves obtained [36] for irradiated $\text{YBa}_2\text{Cu}_3\text{O}_7$ with similar ones for irradiated $\text{Bi}_2\text{Sr}_2\text{CaCu}_2\text{O}_{8+\delta}$ (see, e.g., [37]), it could be concluded that both of them follow a scaling behaviour that could be attributed to a Bose-glass phase [38]. This looks a little surprising because the vortex structures in these materials are very different (tilted vortex lattice for $\text{YBa}_2\text{Cu}_3\text{O}_7$ and crossing vortex lattice for $\text{Bi}_2\text{Sr}_2\text{CaCu}_2\text{O}_{8+\delta}$). This enormous difference of vortex arrays clearly manifests itself in the completely different shape of the melting boundary (elliptical for $\text{YBa}_2\text{Cu}_3\text{O}_7$ and step-wise like for $\text{Bi}_2\text{Sr}_2\text{CaCu}_2\text{O}_{8+\delta}$). Thus, despite of intensive investigation of vortex phases in the presence of columnar defects [39], more detail experimental studies (which are beyond the scope of this study) might be necessary to confirm or demolish the Bose-glass phase in $\text{Bi}_2\text{Sr}_2\text{CaCu}_2\text{O}_{8+\delta}$.

5. Conclusions

We experimentally obtain the phase diagram of the transition between vortex-solid and vortex-liquid in tilted magnetic fields for irradiated $\text{Bi}_2\text{Sr}_2\text{CaCu}_2\text{O}_{8+\delta}$. At low temperatures and at the phase boundary, H_c^{trans} exhibits an unusual concave, hyperbolic-like, dependence on the in-plane magnetic field. We provide an explanation of this unusual behaviour and also a physical picture based on our calculations of the thermodynamic properties for irradiated $\text{Bi}_2\text{Sr}_2\text{CaCu}_2\text{O}_{8+\delta}$.

Note also that the studies of the shape of the vortex-solid melting transition is important in order to control the low vortex-solid low-resistance phase by using external drives, e.g., externally applied currents [40] (which could be useful for some feedback devices).

Acknowledgments

We gratefully acknowledge conversations with Dr A Koshelev, and partial support from the National Security Agency (NSA), Laboratory Physical Science (LPS), Army Research Office (ARO), National Science Foundation (NSF) grant no. EIA-0130383, JSPS-RFBR 06-02-91200,

and Core-to-Core (CTC) program supported by Japan Society for Promotion of Science (JSPS). SS acknowledges support from the Ministry of Science, Culture and Sport of Japan via the grant-in aid for Young Scientists no. 18740224, the EPSRC Advanced Research Fellowship no. EP/D072581/1, and ESF network-programme 'Arrays of Quantum Dots and Josephson Junctions'.

References

- [1] Buzdin A I and Feinberg D 1990 *J. Phys. (Paris)* **51** 1971
Artemenko S N and Kruglov A N 1990 *Phys. Lett. A* **143** 485
Clem J R 1991 *Phys. Rev. B* **43** 7837
- [2] Bulaevskii L and Clem J R 1991 *Phys. Rev. B* **44** 10234
- [3] Huse D A 1992 *Phys. Rev. B* **46** 8621
- [4] Bulaevskii L N, Ledvij M and Kogan V G 1992 *Phys. Rev. B* **46** 366
- [5] Koshelev A E 1999 *Phys. Rev. Lett.* **83** 187
Koshelev A E 2003 *Phys. Rev. B* **68** 094520
Koshelev A E 2004 *Physica C* **408–410** 470
- [6] Savel'ev S E, Mirković J and Kadowaki K 2001 *Phys. Rev. B* **64** 94521
Savel'ev S E, Mirković J and Kadowaki K 2001 *Physica C* **357–360** 597
Savel'ev S E, Mirković J and Kadowaki K 2002 *Physica C* **378–381** 580
Savel'ev S, Mirković J and Nori F 2003 *Physica C* **388** 653
- [7] Buzdin A and Baladié I 2002 *Phys. Rev. Lett.* **88** 147002
- [8] Dodgson M J W 2002 *Phys. Rev. B* **66** 014509
- [9] Tonomura A *et al* 2002 *Phys. Rev. Lett.* **88** 237001
- [10] Matsuda T *et al* 2001 *Science* **294** 2136
- [11] Grigorenko A, Bending S, Tamegai T, Ooi S and Henini M 2001 *Nature* **414** 728
Grigorenko A N, Bending S J, Koshelev A E, Clem J R, Tamegai T and Ooi S 2002 *Phys. Rev. Lett.* **89** 217003
Grigorenko A N, Bending S J, Grigorieva I V, Koshelev A E, Tamegai T and Ooi S 2005 *Phys. Rev. Lett.* **94** 067001
- [12] Tokunaga M, Kobayashi M, Tokunaga Y and Tamegai T 2002 *Phys. Rev. B* **66** 060507 (R)
Vlasko-Vlasov V K, Koshelev A, Welp U, Crabtree G W and Kadowaki K 2002 *Phys. Rev. B* **66** 014523
Yasugaki M, Itaka K, Tokunaga M, Kameda N and Tamegai T 2002 *Phys. Rev. B* **65** 212502
- [13] Cole D, Bending S J, Savel'ev S, Tamegai T and Nori F 2006 *Preprint cond-mat/0605375*
- [14] Tamegai T, Tokunaga M, Matsui M, Kobayashi M and Tokunaga Y 2003 *Physica C* **392** 311
Tamegai T, Matsui M, Tokunaga Y, Kameda N, Aoki H and Tokunaga M 2003 *Int. J. Mod. Phys. B* **17** 3401
- [15] Cole D, Bending S, Savel'ev S, Grigorenko A, Tamegai T and Nori F 2006 *Nature Mater.* **5** 305
Tonomura A 2006 *Nature Mater.* **5** 257
Nori F 2006 *Nature Phys.* **2** 227
- [16] Savel'ev S and Nori F 2006 *Physica C* **437–438** 226
Cole D, Neal J S, Connolly M R, Bending S J, Savel'ev S, Nori F, Tokunaga M and Tamegai T 2006 *Physica C* **437–438** 52
- [17] Savel'ev S and Nori F 2002 *Nature Mater.* **1** 179
Savel'ev S, Marchesoni F and Nori F 2004 *Phys. Rev. Lett.* **92** 160602
Savel'ev S, Marchesoni F and Nori F 2003 *Phys. Rev. Lett.* **91** 010601
Savel'ev S, Marchesoni F and Nori F 2004 *Phys. Rev. E* **70** 061107
Savel'ev S, Marchesoni F and Nori F 2005 *Phys. Rev. E* **71** 011107
Savel'ev S, Marchesoni F and Nori F 2003 *Physica C* **388** 661
Savel'ev S, Marchesoni F, Hänggi P and Nori F 2004 *Europhys. Lett.* **67** 179
Savel'ev S, Marchesoni F, Hänggi P and Nori F 2004 *Phys. Rev. E* **70** 066109

- Savel'ev S, Marchesoni F, Hänggi P and Nori F 2004 *Eur. Phys. J. B* **40** 403
 Marchesoni F, Savel'ev S and Nori F 2006 *Phys. Rev. E* **73** 021102
 Marchesoni F, Savel'ev S and Nori F 2006 *Europhys. Lett.* **73** 513
 Savel'ev S, Marchesoni F, Taloni A and Nori F 2006 *Phys. Rev. E* **74** 021119
- [18] Ooi S, Shibauchi T, Okuda N and Tamegai T 1999 *Phys. Rev. Lett.* **82** 4308
- [19] Ooi S, Shibauchi T, Itaka K, Okuda N and Tamegai T 2000 *Phys. Rev. B* **63** 020501 (R)
- [20] Mirković J, Savel'ev S E, Sugahara E and Kadowaki K 2001 *Phys. Rev. Lett.* **86** 886
 Mirković J, Savel'ev S E, Sugahara E and Kadowaki K 2000 *Physica C* **341** 1181
 Mirković J, Savel'ev S E, Sugahara E and Kadowaki K 2001 *Physica C* **357** 450
 Mirković J, Savel'ev S E, Sugahara E and Kadowaki K 2001 *Physica C* **364** 515
 Kadowaki K, Mirkovic J, Savel'ev S and Sugahara E 2000 *Physica C* **341** 1301
- [21] Tokunaga M, Kishi M, Kameda N, Itaka K and Tamegai T 2002 *Phys. Rev. B* **66** 220501 (R)
- [22] Mirković J, Savel'ev S, Hayama S, Sugahara E and Kadowaki K 2003 *Physica C* **388** 757
- [23] Mirković J, Savel'ev S E, Sugahara E and Kadowaki K 2002 *Phys. Rev. B* **66** 132505
- [24] van der Beek C J, Konczykowski M, Vinokur V M, Li T W, Kes P H and Crabtree G W 1995 *Phys. Rev. Lett.* **74** 1214
- [25] Doyle R A, Seow W S, Yan Y, Campbell A M, Mochiku T, Kadowaki K and Wirth G 1996 *Phys. Rev. Lett.* **77** 1155
 Pastoriza H, Goffman M F, Arribère A and de la Cruz F 1994 *Phys. Rev. Lett.* **72** 2951
- [26] van der Beek C J, Konczykowski M, Samoilov A V, Chikumoto N, Bouffard S and Feigel'man M V 2001 *Phys. Rev. Lett.* **86** 5136
- [27] Blatter G, Geshkenbein V B and Larkin A I 1992 *Phys. Rev. Lett.* **68** 875
- [28] Tachiki M, Iizuka M, Minami K, Tejima S and Nakamura H 2005 *Phys. Rev. B* **71** 134515
 Tominari Y, Kiwa T, Murakami H, Tonouchi M, Wald H, Seidel P and Schneidewind H 2002 *Appl. Phys. Lett.* **80** 3147
 Savel'ev S, Yampol'skii V, Rakhmanov A and Nori F 2005 *Phys. Rev. B* **72** 144515
 Savel'ev S, Yampol'skii V, Rakhmanov A and Nori F 2006 *Physica C* **437–438** 281
 Savel'ev S, Yampol'skii V, Rakhmanov A and Nori F 2006 *Physica C* **445–448** 175
 Savel'ev S, Yampol'skii V, Rakhmanov A and Nori F 2006 *Nature Phys.* **2** 521
 Savel'ev S, Rakhmanov A L and Nori F 2005 *Phys. Rev. Lett.* **94** 157004
 Savel'ev S, Rakhmanov A L and Nori F 2006 *Physica C* **445–448** 180
 Savel'ev S, Yampol'skii V and Nori F 2006 *Phys. Rev. Lett.* **95** 187002
 Savel'ev S, Yampol'skii V and Nori F 2006 *Physica C* **445–448** 183
 Orenstein J 2006 *Nature Phys.* **2** 503
- [29] Mochiku T and Kadowaki K 1993 *Trans. Mater. Res. Soc. Japan A* **19** 349
- [30] Fuchs D T, Zeldov E, Rappaport M, Tamegai T, Ooi S and Shtrikman H 1998 *Nature* **391** 373
- [31] Hayama S, Mirković J, Yamamoto T, Kakeya I and Kadowaki K 2004 *Physica C* **412–414** 478
 Kadowaki K, Hayama S, Kimura K, Mirković J and Savel'ev S 2003 *Physica C* **388** 721
- [32] Tokunaga M, Kishi M, Kameda N, Itaka K and Tamegai T 2002 *Phys. Rev. B* **66** 220501 (R)
- [33] Mirković J, Savel'ev S, Sugahara E and Kadowaki K 2002 *Physica C* **378–381** 428
- [34] Fisher L M *et al* 1995 *Physica C* **245** 231
 Voloshin I F *et al* 1994 *JETP Lett.* **59** 55
- [35] Savelev S E, Fisher L M and Yampolskii V A 1997 *JETP* **85** 507
 Fisher L M, Savel'ev S E and Yampol'skii V A 2000 *Physica B* **284** 735
 Fisher L M *et al* 1997 *Physica C* **278** 169
- [36] Olsson R J, Kwok W K, Paulius L M, Petrean A M, Hofman D J and Crabtree G W 2002 *Phys. Rev. B* **65** 104520
- [37] Ruyter A, Hardy V, Hong N H and Ammor L 2004 *Europhys. Lett.* **68** 571
 Ammor L and Ruyter A 2004 *Physica C* **405** 157

- [38] Nelson D R and Vinokur V M 1993 *Phys. Rev. B* **48** 13060
- [39] Kameda N, Shibauchi T, Tokunaga M, Ooi S, Tamegai T and Konczykowski M 2005 *Phys. Rev. B* **72** 064501
Colson S, van der Beek C J, Konczykowski M, Gaifullin M B, Matsuda Y, Gierlowski P, Li M and Kes P H
2004 *Phys. Rev. B* **69** 180510 (R)
Kameda N, Tokunaga M, Tamegai T, Konczykowski M and Okayasu S 2004 *Phys. Rev. B* **69** 180502 (R)
Menghini M, Fasano Y, de la Cruz F, Banerjee S S, Myasoedov Y, Zeldov E, van der Beek C J, Konczykowski M
and Tamegai T 2003 *Phys. Rev. Lett.* **90** 147001
Banerjee S S *et al* 2003 *Phys. Rev. Lett.* **90** 087004
- [40] Savel'ev S, Cattuto C and Nori F 2003 *Phys. Rev. B* **67** 180509 (R)
Savel'ev S, Mirković J and Kadowaki K 2002 *Physica C* **378–381** 495
Savel'ev S, Nori F, Mirković J and Kadowaki K 2003 *Physica C* **388** 685